

## Electronic Supplementary Information (ESI)

### Gas-Solid Phase Flow Synthesis of the Cu-Co-1, 3, 5-benzenetricarboxylate for Electrocatalytic Oxygen Evolution†

**Author(s):** Hongliang Fan<sup>a#</sup>, Jun Zhao<sup>a#</sup>, Xijun Wei<sup>a</sup>, Huiqiang Liu<sup>a\*</sup>, Ying Xiong<sup>a\*</sup>, Rufang Peng<sup>a</sup>, Bing Wang<sup>a</sup>, Sheng Chu<sup>b</sup>

<sup>a</sup> *State Key Laboratory for Environment-Friendly Energy Materials, Southwest University of Science & Technology, Mianyang 621010, P. R. China;*

<sup>b</sup> *State key Laboratory for Optoelectronics Materials and Technology, Sun Yat-sen University, Guangzhou 510275, China*

\* *The E-mail of corresponding author: [liuhuiqiang@swust.edu.cn](mailto:liuhuiqiang@swust.edu.cn) (H.Liu);*

*xiongying@swust.edu.cn (Y. Xiong)*

## Experimental Section

### *Materials*

$\text{Co}(\text{CH}_3\text{COO})_2 \cdot 4\text{H}_2\text{O}$ ,  $\text{Cu}(\text{NO}_3)_2 \cdot 3\text{H}_2\text{O}$ ,  $\text{H}_3\text{BTC}$  (1,3,5-benzenetricarboxylic acid),  $\text{KOH}$  (95%), C(Conductive Toner), NMP (N-Methyl pyrrolidone) were purchased from Chengdu Kolon Co. PVDF was purchased from Shanghai Maclean Biochemical Co.

### *Synthesis of Cu-Co-BTC*

The target product is produced by transferring a mixture of  $\text{Co}(\text{CH}_3\text{COO})_2 \cdot 4\text{H}_2\text{O}$ ,  $\text{Cu}(\text{NO}_3)_2 \cdot 3\text{H}_2\text{O}$  with  $\text{H}_3\text{BTC}$  (the Molar ratio=1:1:1 and the total mass is 700g), through the inlet into the impact chamber. The mixture is then accelerated to supersonic velocity by a supersonic airflow and the reactant particles collide violently with the target to produce the product. The products are collected every 1 minute by an automatic sampler. Finally, the product is collected after 10 minutes of continuous cycling of the reaction.

The target product was removed from the equipment at 630 g. Here the yield was obtained at about 90 %. The loss was at 10 % because of the residue remained in the equipment.

Removed 10 g from the product and wash 3 times with ultra-pure water, 3 times with ethanol and dry under vacuum at 40° C for 12 h. After three of the above purification operations, a total of 27 g of final product was obtained. Therefore, 10% of the raw material was left over in the original product and the final yield was obtained as 81 %.

### *Preparation of electrodes*

The Cu-Co-BTC, binder and conductive carbon black were mixed and ground at 7:1:2, added to the appropriate amount of N-Methyl pyrrolidone (NMP) solution and stirred until gelatinous, then evenly applied to a  $1 \times 1 \text{ cm}^2$  area of the carbon paper and dried in an oven. The mass difference of the carbon paper before and after the catalyst application was controlled to be about 2.0 mg. Potentials were referenced to a reversible hydrogen electrode (RHE):  $E(\text{RHE}) = E(\text{Ag}/\text{AgCl}) + (0.2 + 0.059 \text{ pH}) \text{ V}$ . The long-term stability tests were performed by a continuous current density of 10

mA cm<sup>-2</sup> was used. All the data presented were corrected for IR losses and carried out at ambient temperature.

### *Characterization*

The phases and crystal structures of the materials were characterized using the powder X-ray diffraction (XRD, Bruker D8 Advance X-ray diffractometer, Co K $\alpha$  radiation,  $\lambda=1.7902$  Å). The morphologies of the samples were observed by field-emission scanning electron microscopy (FESEM, JSM-7800F) and transmission electron microscopy (TEM, JEOL-2100F). FT-IR spectra were recorded on an FT-IR spectrometer using KBr sheets with a resolution of 4 cm<sup>-1</sup> from 400 to 4000 cm<sup>-1</sup> (Thermo Fisher Nicolet 380, USA). X-ray photoelectron spectroscopy (XPS) analyze was conducted on a Thermo Fisher Scientific K-Alpha spectrometer using an Al K $\alpha$  X-ray source (1486.8 eV, 150 W) at a constant analyzer.

### *Theoretical Simulation for structure of Cu-Co-BTC*

The molecular structure of Cu-Co-BTC in Fig.1 was determined by the density functional theory (DFT) calculations and the molecular dynamics (MD) or ab initio molecular dynamics (AIMD) methods. All calculations in this study are based on based on the latest version 5.0 of the quantum chemistry software ORCA and the semi-empirical program GFN2-XTB. GFN-xTB (Geometry, Frequency, Noncovalent, eXtended TB) was proposed by Grimme, it was expected to be able to optimize geometry, frequency calculation, and weak interaction in a very cheap way. The method can be considered relatively reasonable, and can be applied to a large-scale system of thousands of atoms. GFN2-xTB is the second generation of GFN-xTB. It improves the calculation form of the first generation to make it more rigorous, and combines with DFT-D4. It can basically be better than the general semi-empirical method like PM6 in calculating weak interactions of systems. The computational process are as follows:

(1) This study modeled three basic molecules, including Cu(NO<sub>3</sub>)<sub>2</sub>·3H<sub>2</sub>O, Co(CH<sub>3</sub>COO)<sub>2</sub>·4H<sub>2</sub>O and 1, 3, 5-benzenetricarboxylic acid (H<sub>3</sub>BTC). The CAS numbers of the three molecules are 10031-43-3, 6147-53-1 and 554-95-0, respectively. According to the molecular formula and molecular structure, the initial guess structure of the three models was constructed in the Gaussview software. The plane structures

were drawn first, and then adjusted to the spatial shape according to the symmetry of the bond. The bond length button was used to precisely adjust the distance of the original three molecular structures to correspond to the regular bond length table. Coordinating water molecules have little effect on the overall structure, and they also adopt a spatially symmetrical form.

(2) Since the initial structures were adjusted according to the nucleus, it is almost impossible to precisely control the electronic structure. Therefore, generally speaking, the initially constructed model has spatial irrationality and cannot reach the minimum energy condition, in other words it is not stable enough and should be optimized. As shown before, this study used the GFN2-xTB method to optimize the three initial models, and set strict convergence conditions (energy change less than  $1e-6$ , RMS gradient less than  $1e-4$ , MAX gradient less than  $3e-4$ , RMS step size Less than  $2e-3$ , MAX step length is less than  $4e-3$ ), the converged structures were the most stable spatial configurations under this condition (Fig. S1), and the next step can be calculated based on these structures.

(3) According to the optimized molecule (three times of the three molecules were selected separately, since the bound water is in a free state, the hydrogen bond generated was weak enough and would not have a substantial impact on the coordination effect, so the bound water was removed in the subsequent calculations) These structures constructed a series (10) of the initial model of the complex, then AIMD was used for simulation operation, the calculation level kept to GFN2-XTB, the time step was 0.5 fs, the initial temperature was set to ambient temperature 300k, the CSVr temperature control method was used, and the coupling time The constant was 10 fs. The CenterCOM parameters was used to keep the center of mass from shifting during operation, and run 10,000 steps, that is 5 ps.

The constructed 10 initial ligand structures were performed the above molecular dynamics simulation respectively. The simulation generated a trajectory file containing all the process structures. Through the observation the trajectory file, it is necessary to manually screen out reasonable ligand structures. two ligand structures (around 2.5ps and 5ps respectively) was selected. Finally, 20 ligand structures were obtained. This step was relatively computationally expensive and consumed about 3000 core hours.

(4) The reasonable structures of the ligand structures need to be accurately calculated, the two steps of optimization are required next. First, the above 20 ligand

structures were initially optimized by GFN2-xTB level, and the same structures appeared after the optimization. The parameters of MAPEmax=0.0001, BAPEmax=2.5 and eigLmax=0.1 were used to remove redundant structures, and finally 5 ligand structures were left, and higher-level optimization operations were performed on these structures next. In this study, M062X functional and 6-311g(d,p) large basis sets were used for high-level optimization operations (refer to “A brief talk on the selection of DFT functional in quantum chemistry calculations, <http://sobereva.com/272>”) , The M062X functional is robust, practical, and more accurate than semi-empirical methods such as GFN2-xTB. This method was used to fully optimize the five selected ligand structures. Strict convergence conditions were also set during the optimization process (energy change is less than 1e-6, RMS gradient is less than 1e-4, MAX gradient is less than 3e-4, RMS step size is less than 2e-3, MAX step size is less than 4e-3). This step consumed more computing resources, about 5000 core hours.

(5) This step is to analyze the optimization results of M062X/6-311g (d,p), total energy value were extracted for comparison, and the lowest energy structure was determined as the most stable configuration. The configuration was displayed in the Gaussview software, the molecular display type was adjusted, the coordination bond is reconnected, and the reasonable ligand structure diagram was finally obtained (Fig. S2).

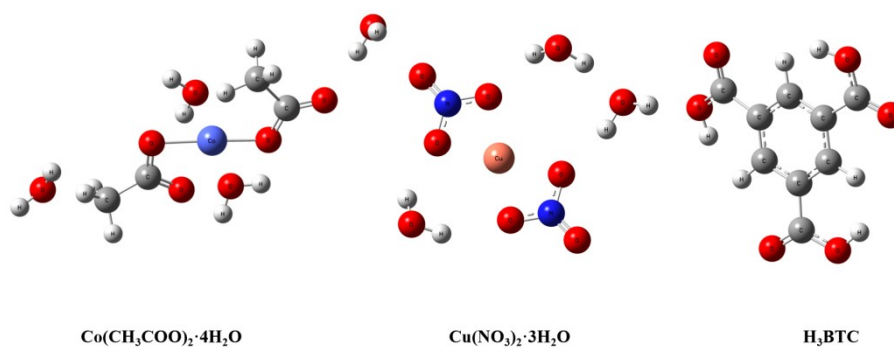


**Fig. S1** The molecular structural formula of  $\text{Co}(\text{CH}_3\text{COO})_2 \cdot 4\text{H}_2\text{O}$ ,  $\text{Cu}(\text{NO}_3)_2 \cdot 3\text{H}_2\text{O}$  and  $\text{H}_3\text{BTC}$ .

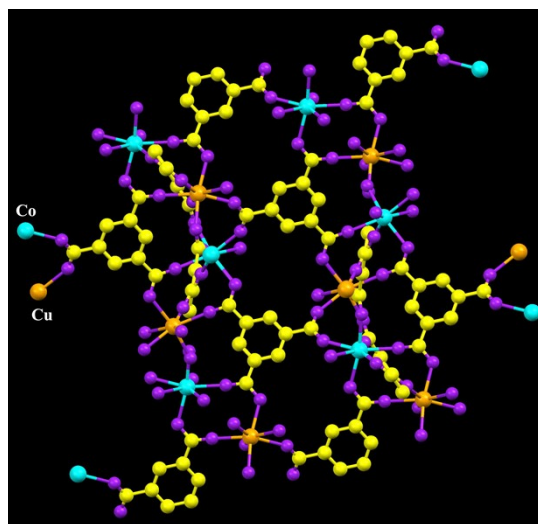


**Fig. S2** The ball and stick diagram of the final coordination structure for Cu-Co-BTC.



**Fig. S3** GSF reaction equipment with key parts highlighted.

The reaction process flow chart of GSF chemical synthesis was shown in **Fig S3**. Reactant particles were transferred into the impacting chamber through the feed port, firstly. Afterward, the particles were accelerated to high velocities (300 m/s) by compressed air (1.5 MPa).

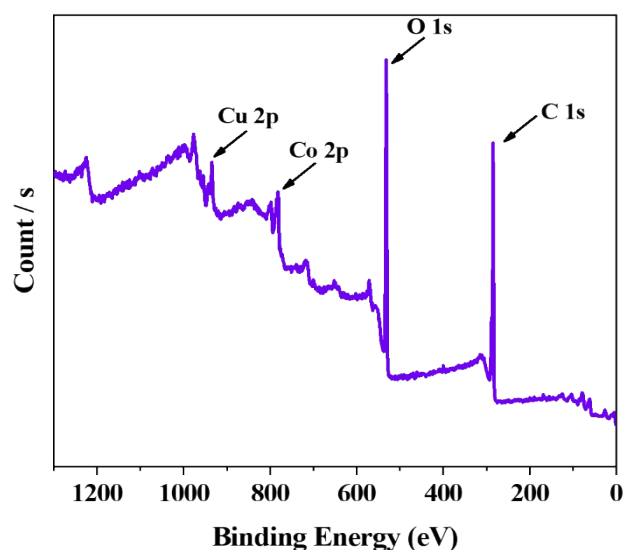


**Fig. S4** The XPS survey spectrum illustrates the presence of C, C, Co and Cu.

**Table S1** Summary of various non-precious metal-based catalysts for OER

Catalysts	Overpotential (mV)		Reference
	at 10 mA cm <sup>-2</sup>		
Fe <sub>2</sub> O <sub>3</sub> /CNT	410		<i>Electrochim. Acta.</i> , <b>2016</b> ,222, 1316–1325
CoP/rGO hybrids	340		<i>Chem. Sci.</i> <b>2016</b> , 7, 1690
γ-Fe <sub>2</sub> O <sub>3</sub> /CNTs	340		<i>J. Mater. Chem. A</i> , <b>2016</b> , 4, 5216
NiCoP/C nanoboxes	330		<i>Angew. Chem. Int. Ed.</i> <b>2017</b> , 56, 3897-3900
M-Co <sub>3</sub> O <sub>4</sub> /NPC	300		<i>Nano-Micro Lett.</i> <b>2018</b> , 10:15
Co <sub>3</sub> O <sub>4</sub> /CoMoO <sub>4</sub>	318		<i>J. Mater. Chem. A</i> , <b>2018</b> , 6, 1639
Co <sub>3</sub> O <sub>4</sub> /Fe <sub>2</sub> O <sub>3</sub>	310		<i>Chem. Eng. J.</i> <b>2019</b> , 355, 336-340
OCNF	291		<i>Adv. Mater. Interfaces</i> , <b>2019</b> , 6, 1900290.
Co-BTC-IMI	360		<i>J. Mater. Chem. A</i> , <b>2020</b> ,8, 22111
Co BTC-rGO	290		<i>Renew. Energ.</i> <b>2020</b> .156.1040
<b>Cu-Co-BTC</b>	<b>239</b>		<b>This work</b>

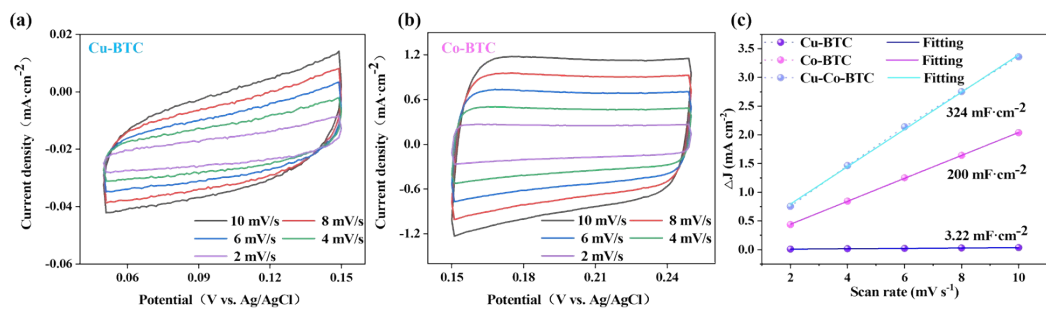


**Fig. S5** (a) the CV curves of Cu-BTC at different scan rates; (a) the CV curves of Co-BTC at different scan rates; (c) the corresponding capacitance currents of Cu-Co-BTC, Cu-BTC, and Co-BTC in 1.0 M KOH.

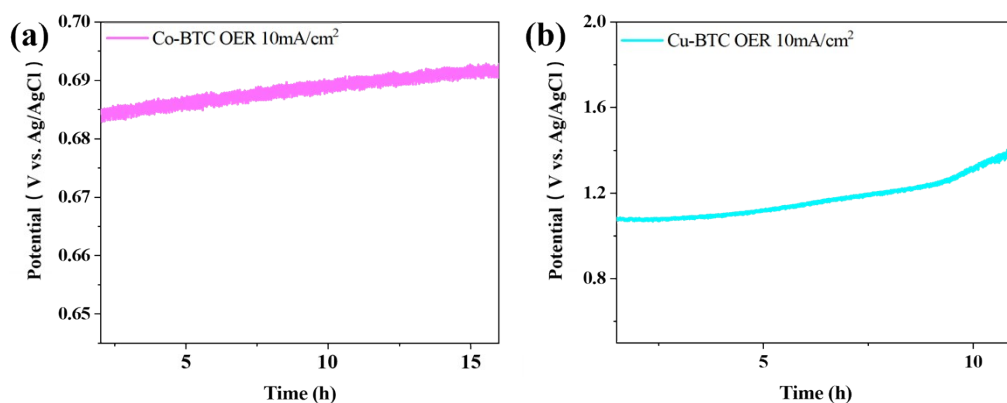


**Fig. S6** Potential versus time (V-t) curves of the OER for Cu/Co-BTC.

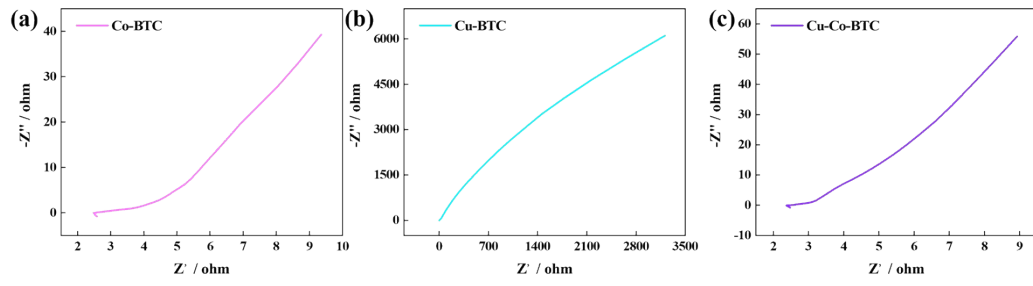


**Fig. S7** EIS results for different electrodes.